Automatic Stress Path Control System for Hollow Cylinder Torsional Testing of Soils

D. WIJEWICKREME, M. UTHAYAKUMAR, AND Y. P. VAID

The deformation response of sands, which are often anisotropic because of their alluvial mode of deposition, under generalized field stress paths that involve principal stress rotation can be assessed systematically in a hollow cylinder torsional test. In this test, the specimen is subjected to four independently controlled surface tractions that allow loading under a prescribed stress or strain path. Pursuit of such stress or strain paths requires the use of simultaneous increments to more than one stress or strain component. A computer feedback control system for carrying out complex stress path tests in a hollow cylinder torsional device is described. As opposed to the generally adopted sequential loading and transducer signal readout methods, simultaneous control of all four external surface tractions and the synchronous digital readout of all transducers is carried out. This is accomplished by using four stepper motor-driven pneumatic regulators and a system of parallel analog-to-digital converters in which the number of converters equals the number of transducer signals monitored. The system allows the performance of totally stress-controlled or strain-controlled tests. In strain-controlled tests, more than one strain component can be positively controlled. The strain-controlling option permits the accurate capture of the postpeak strain softening characteristics of loose saturated sands by overcoming undesirable runaway strains inevitable in stress-controlled tests. Thus the behavior of soil can be assessed not only under controlled stress paths but also under controlled strain paths. The details of the control system are described, and its capabilities are illustrated by using experimental data from complex stress path tests.

In soil modeling, anisotropy has generally been disregarded. Alluvial soils, however, are typically anisotropic in their mechanical behavior. Consequently, their deformation response depends not only on the magnitudes of stress increments but also on their directions in relation to the orientation of bedding planes. The ability to model the behaviors of real soils is essential for any meaningful prediction of the deformations that would be found under complex loading conditions (*1*).

Important problems in which the anisotropic response manifests itself and should require considerations in design are earthquakes and the wave loadings of soils. This was clearly recognized during characterization of the Erksak sand of the Molikpaq caisson-retained island in the Canadian Arctic, which suffered damage during an ice-loading event (*2,3*). In these and several other field problems involving water-deposited soils, principal stress directions rotate during loading, thereby invoking deformations even if the stress magnitudes remain constant.

D. Wijewickreme, Golder Associates, Ltd., #500-4260, Still Creek Drive, Burnaby, British Columbia V5C 6C6, Canada. M. Uthayakumar and Y. P. Vaid, Department of Civil Engineering, 2324 Main Mall, University of British Columbia, Vancouver, British Columbia V6T 1W5, Canada.

The hollow cylinder torsional (HCT) device has been employed by several researchers, for example, Hight et al. (*4*), Vaid et al. (*5*), Saada and Baah (*6*), Lade (*7*), and Miura (*8*), to study the direction-dependent (anisotropic) behaviors of soils together with the effects of principal stress rotation. In this test, a hollow cylindrical soil specimen is subjected to four surface tractions: vertical load (W), torque about the vertical axis (T), and internal (P_i) and external (P_e) cell pressures. These tractions give rise to average vertical, radial, circumferential, and shear stresses (σ'_z, σ'_r, σ'_θ, and $\tau_{z\theta}$, respectively) in the specimen, which depend, in addition, on the geometry of the specimen. In this manner, the HCT device permits an independent control of the magnitudes of the three principal stresses, the major, intermediate, and minor effective principal stresses (σ'_1, σ'_2, and σ'_3, respectively), and the direction of σ'_1 with respect to the vertical deposition direction of the soil specimen α_σ.

A general stress path loading in the HCT test necessitates simultaneous variations in more than one surface traction. Clearly, some form of automatic control is required if the desired stress path is to be followed faithfully. This involves measuring the current stress state and commanding the control system to alter the surface tractions so as to march to the final stress state in several small increments along the prescribed stress path. The targeted stress state at the end of each increment can be ensured by performing one or more iterations.

Manual control of four surface tractions simultaneously in a hollow cylindrical specimen is extremely cumbersome. To overcome such difficulties, several automatic stress path control systems have been developed. The earliest of such devices is the pneumatic analog stress path control system of Saada and Baah (*6*). Further advances in automatic stress path testing have also been made by using direct current servo-controlled systems in hollow cylinder torsional and cuboidal shear testing devices (*4,9*).

The most advanced stress path control system used in HCT testing appears to be that used by Shibuya (*10*). Shibuya's system uses a computer-controlled stepper motor system instead of servo controls. It, however, is a purely stress-controlled system and, therefore, does not permit prescribed displacements to be imposed on the specimen. The displacement control feature is of utmost importance in the assessment of the liquefaction potential of loose contractive sands that undergo strain softening on undrained loading. A stress control system is not suitable for measuring postpeak behavior (such as residual strength) because of the specimen-apparatus interaction (*11*) together with the inability to adhere to the prescribed stress path. Furthermore, concurrent, and not sequential, measurement of all tractions is essential to circumvent phase delay among measured tractions at a given time. This is

necessary if the tractions change rapidly or the specimen is deforming fast, requiring an update of the geometry that intimately links the tractions to the stresses. Shibuya's (*10*) system takes only sequential measurements of signals and is thus prone to phase delays. This may cause the actual stress path imposed to deviate significantly from that desired.

Microcomputer-based data acquisition systems allow faster data acquisition and feedback control. They allow the virtually simultaneous execution of the control step once the data have been scanned. This paper describes an automatic microcomputer [personal computer (PC)]-controlled loading system for HCT tests on soils. The system is designed to read all transducers concurrently to avoid any phase delay in computing the incremental traction changes to be applied. It has also been designed with capabilities of displacement control on two components of displacement (vertical and rotational). This enables both drained and undrained behaviors to be investigated under either stress or strain path control. The features and capabilities of the control system are described, and typical results are presented to illustrate its stress or stress or displacement control capabilities along prescribed stress or strain paths.

UBC HOLLOW CYLINDER TORSIONAL APPARATUS

A detailed description of the University of British Columbia (UBC) HCT shear device has been presented by Vaid et al. (*5*). The cylindrical soil specimen has an external diameter of 15.2 cm, an internal diameter of 10.2 cm, and a height of 30.0 cm. This geometry was selected after careful consideration to minimize stress nonuniformities within the wall of the specimen (*2,12*). A schematic illustration of the apparatus is shown in Figure 1.

Four deformation components are measured by using suitable transducers: vertical displacement (specimen height change), rotational displacement about the vertical axis, volume change of the specimen, and volume change of the inner chamber. These measurements enable computation of the vertical, radial, circumferential, and shear strain components (ϵ_z, ϵ_r, ϵ_θ, and $\gamma_{z\theta}$, respectively) associated with the stress components σ'_z, σ'_r, σ'_θ, and $\tau_{z\theta}$, respectively, and, in turn, the major, intermediate, and minor principal strains (ϵ_1, ϵ_2, and ϵ_3, respectively). The stress components at a given instant are calculated from the values of four surface tractions, W, T, P_i, and P_e. These, together with pore water pres-

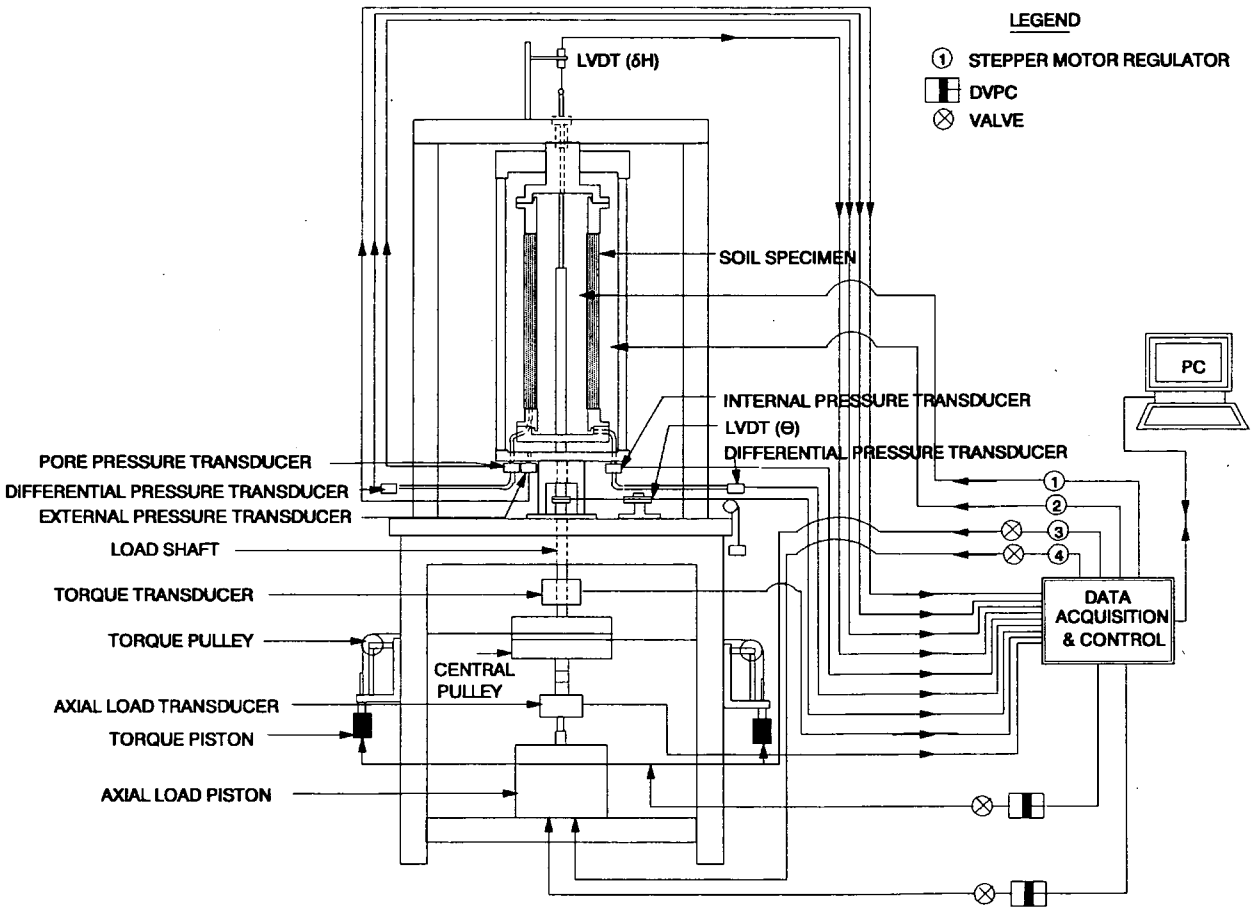

FIGURE 1 HCT apparatus and control system.

sure, are measured by using appropriate transducers. Stresses can be measured with a resolution of 0.25 kPa, and strains can be measured with a resolution of 5×10^{-4}.

NEW AUTOMATIC CONTROL SYSTEM

A schematic layout of the control system is shown in Figure 1, together with its association with the apparatus. The system basically consists of a microcomputer and a monitoring (data acquisition) and control interface unit. Transducer signals are conditioned and scaled to ±2 V for full-scale output before monitoring by the data acquisition system.

Stress-Controlled Loading

Stress-controlled loading is achieved by four motor-set precision regulators. The regulators have a range of 0 to 700 kPa. In response to a logic sequence from the computer, a control chip outputs a series of square pulses to the stepper motors. These pulses turn the motors and increase or decrease the pressure. The logic sequence from the computer contains information pertaining to the direction of rotation and the number of pulses needed to achieve each pressure change. A single pulse advances the motor-set regulator by one step, and approximately 12 to 13 pulses are needed to alter the pressure by 1 kPa. Because the motors are operated by a computer-controlled feedback action, the system does not suffer from limitations such as slack in gears. These regulator motors can be set to alter pressures at a rate of approximately 3.0 to 14 kPa/sec. Slower rates are clearly needed to ensure full drainage in drained tests.

Displacement Controlled Loading

Displacement controlled loading is achieved by two digital volume pressure controllers (DVPCs) connected to vertical and torsional loading pistons. A DVPC consists essentially of a water cylinder and a piston. The piston is attached to a ball screw that is advanced by a stepper motor (*13*). Depending on the amount of motor rotation, diameter of the cylinder, and pitch of the ball screw, predetermined volume increments of water can be delivered or extracted from the loading pistons, which translates directly into the desired strain increment. For displacement control the loading pistons must be saturated with water.

Data Acquisition

All transducer channels are read concurrently, as opposed to being read by the generally adopted sequential readout methods (Figure 2). The analog voltage signal from each transducer is integrated over a 50-msec period by an analog circuit, and its average value is obtained. This is then digitized by its own analog-to-digital (A/D) converter, and the results are temporarily stored in a memory chip for later retrieval by the microcomputer. The digital output after A/D conversion yields a number from 0 to ±40,000 (approximately 16 bits in binary) corresponding to an analog voltage range of 0 to ±2.0. This amounts to a resolution of the measuring system on the order of 0.1 mV.

CAPABILITIES OF UBC HCT WITH CONTROL SYSTEM

Average stresses and strains in the HCT specimen in terms of surface tractions and measured deformation are given by the following expressions (*2*):

$$\sigma_z = \frac{W + \pi(P_e r_e^2 - P_i r_i^2)}{\pi(r_e^2 - r_i^2)} \tag{1}$$

$$\sigma_r = \frac{(P_e r_e^2 - P_i r_i^2)}{r_e^2 - r_i^2} - \frac{2(P_e - P_i) r_e^2 r_i^2 \ln(r_e/r_i)}{(r_e^2 - r_i^2)^2} \tag{2}$$

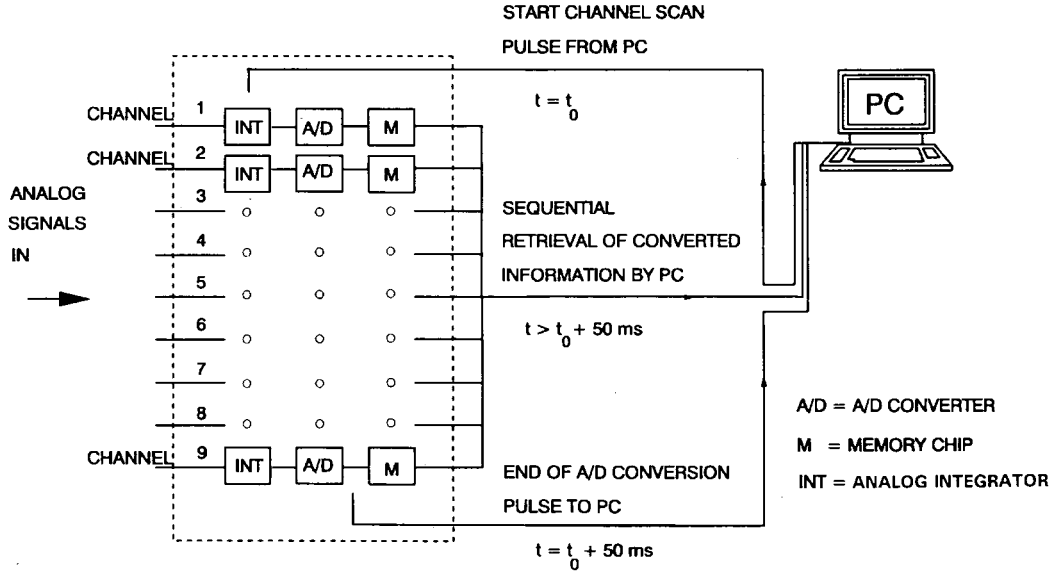

FIGURE 2 Data acquisition process (t_0 is time zero).

$$\sigma_0 = \frac{(P_e r_e^2 - P_i r_i^2)}{r_e^2 - r_i^2} + \frac{2(P_e - P_i) r_e^2 r_i^2 \ln(r_e/r_i)}{(r_e^2 - r_i^2)^2} \quad (3)$$

$$\tau_{z\theta} = \frac{4T(r_e^3 - r_i^3)}{3\pi(r_e^4 - r_i^4)(r_e^2 - r_i^2)} \quad (4)$$

$$\epsilon_z = -\Delta H/H \quad (5)$$

$$\epsilon_r = \frac{-(\Delta r_e - \Delta r_i)}{r_e - r_i} \quad (6)$$

$$\epsilon_\theta = \frac{-(\Delta r_e + \Delta r_i)}{r_e + r_i} \quad (7)$$

$$\gamma_{z\theta} = \frac{2\Delta\theta(r_e^3 - r_i^3)}{3H(r_e^2 - r_i^2)} \quad (8)$$

where

r_e and r_i = the external and internal specimen radii, respectively;

ΔH, Δr_e, and Δr_i = the change (current − initial) in height and in external and internal radii, respectively, of the specimen; and

$\Delta\theta$ = the angular displacement of the base relative to the top of the specimen.

The results from HCT tests are generally examined in terms of the effective mean normal stress (σ'_m), maximum shear stress (or the effective principal stress ratio $R = \sigma'_1/\sigma'_3$), intermediate stress magnitude σ'_2 (specified by the intermediate principal stress parameter b, where $b = [(\sigma'_2 - \sigma'_3)/(\sigma'_1 - \sigma'_3)]$), and inclination α_σ of σ'_1 to the vertical. This set of stress parameters is equivalent to the set defined by Equations 1 to 4, in that one set uniquely determines the other.

Inverse relationships that relate σ'_m, R or $(\sigma'_1 - \sigma'_3)$, b, and α_σ to surface tractions can be easily established. This permits any stress path in σ'_m, $(\sigma'_1 - \sigma'_3)$ or R, b, and α_σ space to be followed by simultaneous incremental changes in surface traction by the control system.

Stress-Controlled Loading

The algorithm used for closed-loop controlled-stress path testing is presented in Figure 3. The software consists of the following major components:

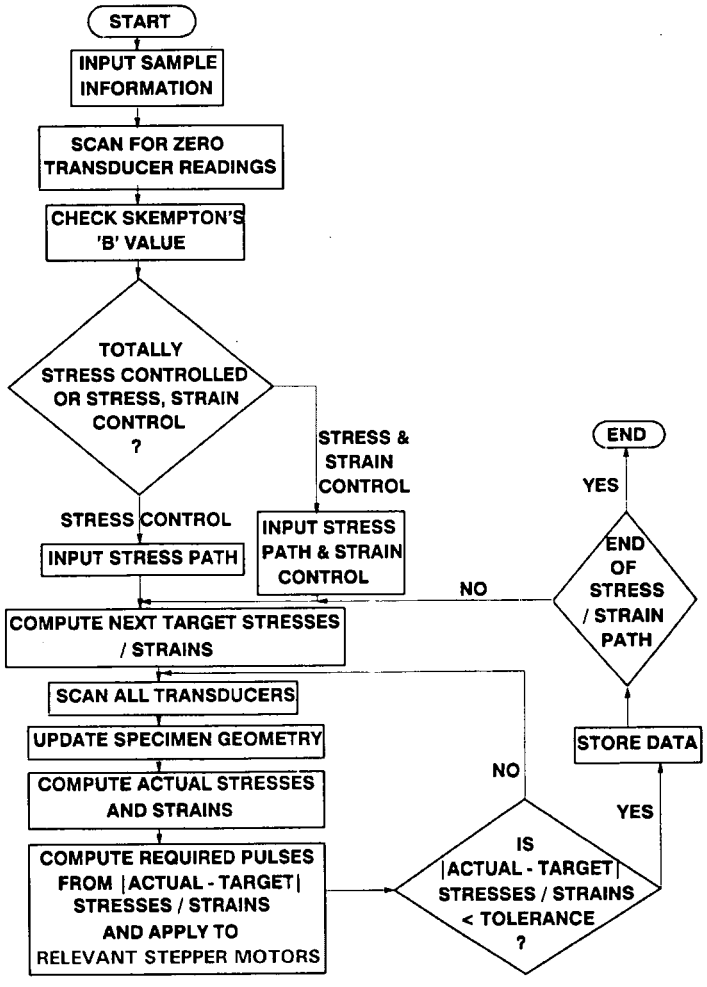

FIGURE 3 Flow chart for stress or strain path control.

- Input of initial information, that is, specimen dimensions, reference readings for transducers, and so on;
- Skempton's *B*-value check for saturation;
- Input of the stress path to be followed (including the consolidation phase);
- Control of surface tractions;
- Check for deformation equilibrium;
- Data storage; and
- Application of next loading increment.

Once the initial information is fed into the computer, the specimen is loaded hydrostatically (undrained) in an incremental manner for a saturation check. After the saturation check, the computer reads a file containing information on the desired stress path to be followed. (No distinction is made between the consolidation and shear loading phases for this purpose; both are treated as specific stress paths.) This information contains the σ'_m, R or $(\sigma'_1 - \sigma'_3)$, b, and α_σ coordinates of the key turning points in the stress path or along a straight-line path if desired. The number of increments needed to reach the target stress state is prescribed so that the computer can linearly interpolate and determine the intermediate stress states.

A pressure control routine governs the incremental changes in surface tractions for moving the stress state of the specimen along the prescribed stress path. To apply a small load increment, the target values of the four surface tractions (i.e., external and internal pressures, torque, and vertical load) are calculated. The differences between the current and the target surface tractions are then computed, and the numbers of pulses to each motor set regulator required to bridge the difference are calculated. The pulses are sent to the stepper motors simultaneously so that all regulators are activated together. Each surface traction is adjusted until the tractions achieved are within a given tolerance from the target values. The tolerance for the surface tractions is stipulated so that no stress component deviates more than 0.5 kPa from its target value.

After the increment of loading, the deformation equilibrium of the specimen is checked by monitoring the deformations of the specimen with time. The specimen is considered to be in equilibrium if the change in any strain component in 1 min does not exceed 5 percent of the change in the same strain component in the previous 1 min. If the specimen has not reached deformation equilibrium, monitoring is continued. Because the specimen dimensions are updated each time that the transducers are read, the control decisions could be based on the most recent configuration of the specimen. When deformation equilibrium is reached, data pertaining to the current stress state are stored in a data file and the next loading increment is applied in a similar manner until the final target stress state of the prescribed stress path is achieved.

Displacement-Controlled Loading

As illustrated in Figure 1, the strain components ϵ_z and $\gamma_{z\theta}$ can be directly controlled. An additional DVPC that enables direct control of the volumetric strain (ϵ_v) of the specimen can be added. The addition of a fourth DVPC connected to the inner chamber could, in principle, permit control of all strain components.

Direct control of any of the strain components ϵ_z, $\gamma_{z\theta}$, or ϵ_v is accomplished by the control program in a manner similar to that for stress control. To impose a given strain increment, the desired numbers of pulses are computed and transmitted to the stepper motors of the relevant DVPC. The DVPC then injects or withdraws water from the loading pistons, pore space, or inner chamber, depending on the strain component to be controlled. The targeted strain increments are then ensured by using the feedback loop similar to that used for the targeted stresses.

It is possible to carry out stress path tests under a mixed stress and strain control. For example, undrained static loading at constant α_σ, total mean normal stress (σ_m), and b can be carried out by imposing a constant rate of $\gamma_{z\theta}$ and controlling W, P_e, and P_i. Alternatively, ϵ_z may be increased at a constant rate and tractions P_e, P_i, and T can be controlled.

SYSTEM PERFORMANCE AND TYPICAL RESULTS

Drained Stress-Controlled Loading

Figure 4 shows results for a loose specimen of sand [relative density (D_r) = 30 percent and hydrostatically consolidated to σ'_{mc} = 300 kPa] shear loaded under constant σ'_m = 300 kPa and b = 0.5 along a linear stress path with simultaneous variation of R and α_σ(R-α_σ path) until α_σ = 45 degrees and R = 2. Thereafter the loading is continued at constant σ'_m, b, and R and only α_σ is increased (α_σ path).

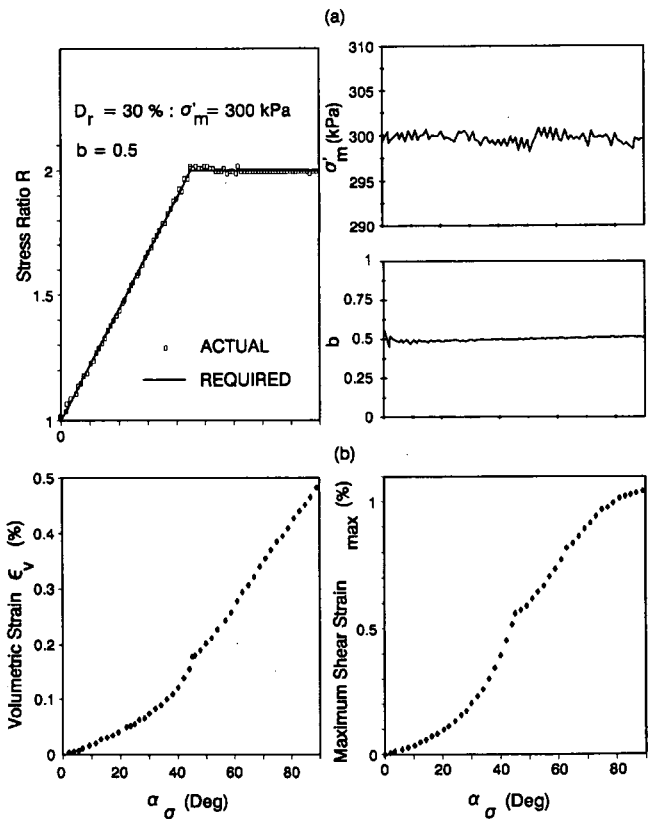

FIGURE 4 Response of a loose sand under static stress-controlled drained stress path: (*a*) comparison between the desired and actually imposed stress path; (*b*) sand deformation under principal stress rotation only.

Excellent simulation of the desired stress path by the control system may be noted in Figure 4(*a*). In Figure 4(*b*) the development of volumetric strain and maximum shear are illustrated as functions of α_σ. In the range of α_σ from 45 to 90 degrees, even though the stress state σ'_m, R, and b (or σ'_1, σ'_2, and σ'_3) remain constant, considerable deformation develops because of principal stress rotation only. This clearly shows that the deformation response of loose sand is anisotropic.

Undrained Static Loading at Constant α_σ

Results for the undrained loading of a loose sand initially hydrostatically consolidated to σ'_{mc} = 200 kPa but sheared with σ'_1 inclined at 60 degrees to the bedding planes are shown in Figure 5(*a*) and (*b*). During the shearing process, σ_m, α_σ, and b were held constant. It may be noted that the desired stress path σ_m = 200 kPa and b = 0 is very closely simulated.

Figure 5(*c*) shows effective stress paths in a series of tests on identical specimens of a loose sand. These consisted of tests with σ'_1 inclined at constant values of 0, 30, 45, 60, and 90 degrees to the bedding planes. Soil behavior may be noted to undergo progressive softening as α_σ values increase from 0 to 90 degrees. The sand is not strain softening for α_σ = 0 degrees, but manifests this behavior to a greater degree as α_σ increases. It may be noted that the strain softening features, together with the turnaround at the phase transformation at which the pore pressure changes from positive to negative, are properly captured by exercising displacement control on $\gamma_{z\theta}$ only. In a purely stress-controlled loaded system it is not possible to capture sand behavior after the occurrence of a maximum in $(\sigma'_1 - \sigma'_3)$, and the true postpeak behavior cannot be measured because of specimen-apparatus interaction (*11*).

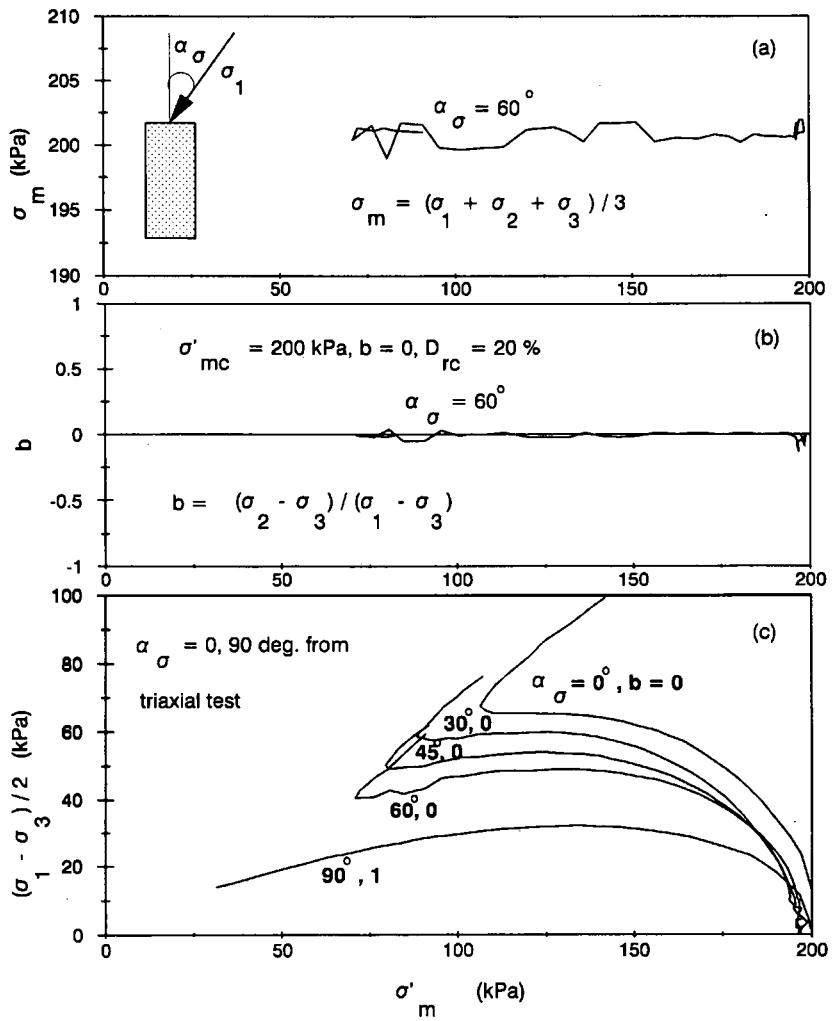

FIGURE 5 Response of a loose sand under static stress- or strain-controlled undrained stress path: (*a* and *b*) comparison between desired and actually imposed stress paths; (*c*) anisotropic response of loose sand.

Undrained Cyclic Loading at Constant $(\sigma_1 - \sigma_3)$ Amplitude

Figure 6 shows the results for cyclic undrained loading of a loose sand with several cycles of constant $(\sigma_1' - \sigma_3')$ amplitude. Cyclic loading was carried out with σ_1' suffering jump rotations of 90 degrees between directions inclined at 45 degrees to the bedding planes and with values of σ_m and b held constant.

Once again the control system may be observed to impose the desired stress path very faithfully. Such a loading is different from conventional undrained cyclic triaxial tests in which σ_1' suffers 90 degrees of jump rotation between $\alpha_\sigma = 0$ and 90 degrees with σ_m not constant and $b = 0$ during one-half of the cycle and $b = 1$ during the other half of the cycle. The knowledge of the directional behavior is of great importance in assessing the full spectrum of the cyclic loading response of sand under identical amplitudes of $(\sigma_1' - \sigma_3')$.

SUMMARY AND CONCLUSIONS

A computer feedback-controlled system was developed to carry out stress path- or strain path-controlled tests in an HCT shear device. In contrast to the generally available sequential channel readout methods involving phase delays, the new system acquires data by scanning all load and displacement transducers in a synchronous manner. This system, therefore, eliminates the potential errors in the calculated load or displacement increment requirements owing to the transducer readout phase lag inherent in previously used automatic test control systems.

In addition, the system is designed to have the ability to impose either stress- or strain-controlled loading or a combination thereof. This feature enables capture of the true postpeak stress-strain undrained response of sand, including strain softening leading to liquefaction or limited liquefaction under principal stress rotation.

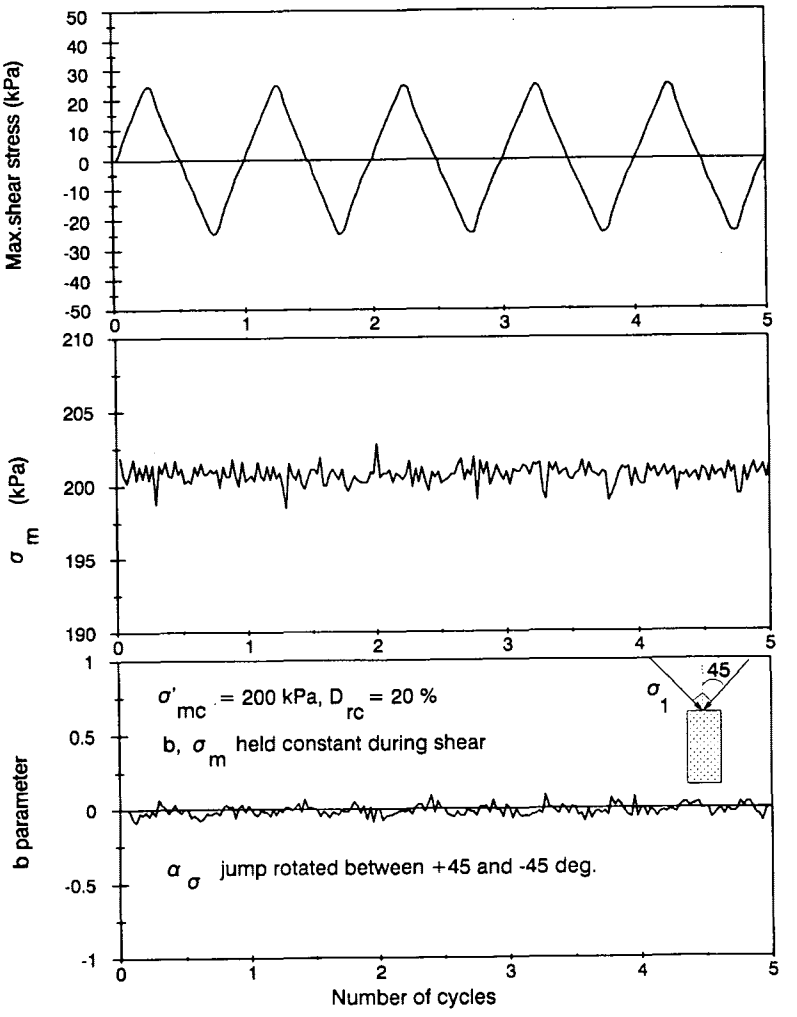

FIGURE 6 Undrained cyclic loading of sand at constant $(\sigma_1 - \sigma_3)$ amplitude with σ_m and b held constant and jump rotated between ± 45 degrees.

The system's capabilities are demonstrated by the results of drained and undrained tests carried out under prescribed stress- or strain-controlled loading conditions. Although the applicability of the system has been demonstrated for conducting tests in an HCT shear device, the system and its concepts can be conveniently adapted to carry out tests in any device that requires feedback control of multiple stress or strain components.

ACKNOWLEDGMENTS

This research was supported by a grant from the Natural Science and Engineering Council of Canada. The assistance of Kelly Lamb in preparing the manuscript is gratefully acknowledged.

REFERENCES

1. Saada, A., and G. Bianchini, eds. Constitutive Equations for Granular Non-Cohesive Soils. *Proc., International Workshop on Constitutive Equations for Granular Non-Cohesive Soils*, July 1987, Cleveland, Ohio, A. A. Balkema, Rotterdam, 1989.
2. Sayao, A. S. F. *Behaviour of Sands Under General Stress Paths in the Hollow Cylinder Torsional Device*. Ph.D. thesis. Department of Civil Engineering, University of British Columbia, Vancouver, British Columbia, Canada, 1989.
3. Salgado, F. M. G. A. *Analysis Procedures for Caisson-Retained Island Type Structures*. Ph.D. thesis. Department of Civil Engineering, University of British Columbia, Vancouver, British Columbia, Canada, 1990.
4. Hight, D. W., A. Gens, and M. J. Symes. The Development of a New Hollow Cylinder Apparatus for Investigating the Effects of Principal Stress Rotation in Soils. *Geotechnique*, Vol. 33, No. 4, 1983, pp. 355–383.
5. Vaid, Y. P., A. Sayao, E. Hou, and D. Negussey. Generalized Stress-Path-Dependent Soil Behaviour with a New Hollow Cylinder Torsional Apparatus. *Canadian Geotechnical Journal*, Vol. 27, 1990, pp. 601–616.
6. Saada, A. S., and A. K. Baah. Deformations and Failure of a Cross-Anisotropic Clay Under Combined Stresses. *Proc., 3rd Pan-American Conference on Soil Mechanics and Foundation Engineering*, Vol. 1, 1967.
7. Lade, P. V. *Torsion Shear Apparatus for Soil Testing. Laboratory Shear Strength of Soil*, STP 740 (R. N. Yong and F. C. Townsend, eds.). ASTM, Philadelphia, 1981, pp. 145–163.
8. Miura, K. *Study on the Deformation Behaviour of Anisotropic Sand Under Principal Stress Axes Rotation*. Ph.D. thesis. Hokkaido University, Hokkaido, Japan, 1985.
9. Sivakugan, N., J. Chameau, R. D. Holtz, and A. G. Altschaeffl. Servo-Controlled Cuboidal Shear Device. *Geotechnical Testing Journal*, ASTM, Vol. 11, No. 2, June 1988, pp. 119–124.
10. Shibuya, S. A Servo System for Hollow Cylinder Torsional Testing of Soils. *Geotechnial Testing Journal*, ASTM, Vol. 11, No. 2, 1988, pp. 109–118.
11. Chern, J. C. Undrained Response of Saturated Sands with Emphasis on Liquefaction and Cyclic Mobility. Ph.D. thesis. Department of Civil Engineering, University of British Columbia, Vancouver, British Columbia, Canada, 1985.
12. Wijewickreme, D., and Y. P. Vaid. Stress Nonuniformities in Hollow Cylinder Torsional Shear Device. *Geotechnical Testing Journal*, ASTM Vol. 14, No. 4, 1991, pp. 349–362.
13. Menzies, B. K. A Computer Controlled Hydraulic Triaxial Testing System. *Advanced Triaxial Testing of Soil and Rock*, STP 977. ASTM, Philadelphia, 1988, pp. 82–94.